Journal of the Serbian Society for Computational Mechanics / Vol. 19 / No. 2, 2025 / pp 32-47 / original paper
(10.24874/jsscm.2025.19.02.03)

CRITICAL STRESS EVALUATION IN RECTANGULAR CORRODED PIPE TEES UNDER INTERNAL PRESSURE

Mansour Boudjelid[1] [0009-0002-5061-816X], Aicha Metehri[1*] [0009-0002-2221-6833] Belaïd Mechab[1] [0009-0000-7483-5527] and Bel Abbes Bachir Bouiadjra[1] [0000-0002-1925-7194]

[1] University of Sidi Bel Abbes, Faculty of Technology / Mechanical Engineering Department, Laboratory of Physical Mechanics of Materials, Sidi Bel Abbès, Algeria.
e-mail: mansourcm@yahoo.fr ; ametehri@yahoo.com ; bmechab@yahoo.fr ; bachirbou@yahoo.fr
*corresponding author

Abstract

The objective of this study is to investigate the structural response of a steel pipe reducing tee containing a rectangular corrosion defect beneath the crotch region under internal pressure loading. Finite element simulations were conducted to evaluate residual stress distributions resulting from imposed boundary conditions, with particular emphasis on the combined influence of the defect and crotch geometry—both recognized as critical sites for stress concentration and crack initiation. A series of parametric studies examined the effects of internal pressure, defect dimensions, crotch radius, crotch thickness, and the interaction between defect depth and spacing. These parameters were selected to represent conditions of practical relevance in the assessment and design of pressure-bearing pipe connections. The analyses reveal that the presence of a corrosion defect significantly increases stress intensities in the crotch region, whereas increasing both crotch thickness and radius markedly reduces peak stress magnitudes. Furthermore, the interaction between defect depth and spacing exerts a decisive influence on crack propagation. These findings highlight the importance of accurate defect characterization and strategically engineered reinforcement measures to enhance reliability and extend the service life of pipe tee connections.

Keywords: Pipe reducing tee, Crotch region, Residual stress, Rectangular corrosion defect, Defect size, Finite Element Analysis (FEA), Corrosion defect.

1. Introduction

In contemporary society, pipelines are among the most crucial infrastructures, facilitating the large-scale movement of vital fluids such as crude oil, natural gas, refined products, industrial water, and various chemicals. Their significance transcends their technical function, serving as a cornerstone for energy security, economic growth, and consistent supply. Compared to traditional transportation methods like road tankers or shipping, pipelines provide a continuous, cost-effective, and relatively safe way to transport large quantities of fluids over long distances. Their energy efficiency, dependability, and minimal environmental impact further underscore their

essential role in global energy and industrial systems (Mechab et al. 2020; Mechab et al. 2018; Mechab et al. 2014).

However, pipelines are susceptible to harsh operating conditions that can undermine their mechanical integrity and shorten their lifespan. Internally, they endure pressure from the transported fluid, which creates circumferential (hoop), longitudinal, and radial stresses within the pipe wall. Externally, they are affected by loads from the surrounding soil, surface traffic, geotechnical or seismic movements, while temperature changes due to fluid or environmental conditions introduce additional stresses (Mechab et al. 2011).

Internal corrosion is often linked to the presence of water, CO_2, H_2S, or other corrosive substances within the transported fluid, whereas external corrosion is caused by humidity, soil electrochemical properties, or the failure of protective coatings. Localized corrosion, such as pitting or cavities, is particularly concerning as it reduces wall thickness and acts as a stress concentrator, quickly leading to crack initiation (Metehri et al. 2024a; Wasim et al. 2022; Chen et al. 2020; Kim et al. 2021; Zhao et al. 2024). Stress corrosion cracking, resulting from the combined effect of a corrosive environment and mechanical stresses, also hastens the fissuring process (Metehri et al. 2024b). Simultaneously, erosion-corrosion, driven by turbulent flow or the transport of solid particles, results in the gradual thinning of the walls. The consequences of such degradation are numerous (Huang et al. 2023; Kim et al. 2002; Tang et al. 2020; Taylor et al. 2016; Wang et al. 2021).

Numerical analysis, especially the finite element method, has gained importance as it allows for the simulation of stress distributions, identification of critical areas, and evaluation of structural behavior under different loading conditions (Zhao et al. 2018; Maachou et al. 2025; Fezazi et al. 2021; Mechab et al. 2025; Serier et al. 2016; Ibrahim et al. 2018; Talbi et al. 2024; Salem et al. 2024). Preventive maintenance strategies, ranging from localized repairs to the replacement of entire sections, ensure service continuity and operational safety. Despite these advancements, pipelines remain vulnerable to complex scenarios where multiple degradation mechanisms interact simultaneously (Salem et al. 2019). Corrosion, particularly when combined with high mechanical stresses, is one of the most severe issues. The interaction between defect depth, spacing, local geometry (such as elbows, tees, and welds), and internal pressure plays a crucial role in the development of equivalent stresses and rupture risk. Numerical simulation, therefore, becomes an essential tool for analyzing these interactions, predicting residual service life, and guiding prevention strategies. While pipelines are vital infrastructures, mechanical stresses and corrosion phenomena present challenges to their reliability. Understanding and managing these mechanisms is crucial to ensure safety, extend service life, and mitigate economic and environmental impacts. The present study is situated within this perspective, aiming to deepen the analysis of the interactions between geometric defects, corrosion, and mechanical loading, through a numerical approach that enables a more accurate evaluation of stress distribution and the identification of critical areas.

2. Numerical modeling and FEM

In this study, a three-dimensional finite element model (FEM) was developed using the commercial software ABAQUS (2024) to analyze the circumferential, radial, and longitudinal stress fields induced in a reducing tee with an external rectangular defect. The component investigated was an ASME B16.9 reducing tee, consisting of a main run and a reduced branch connection. The finite element methodology and model formulation were developed and validated in our previous publications (Metehri et al. 2025; Metehri et al. 2009; Metehri et al. 2024c).

2.1. Geometrical and Materials Models

A welded reducing tee, conforming to ASTM A106 Grade B and specified in ASME B16.9, was examined. This component featured one inlet and two outlets of varying diameters, measuring 168.3 mm and 114.3 mm, with center-to-end distances of 143 mm and 130 mm, respectively, and a wall thickness of 10.97 mm. A corrosion defect was identified near the smaller outlet on the run, with dimensions of 50 × 40 × 10 mm. Figures 1 and 2 illustrate the corroded geometry and study paths, while Table 1 provides the detailed dimensions.

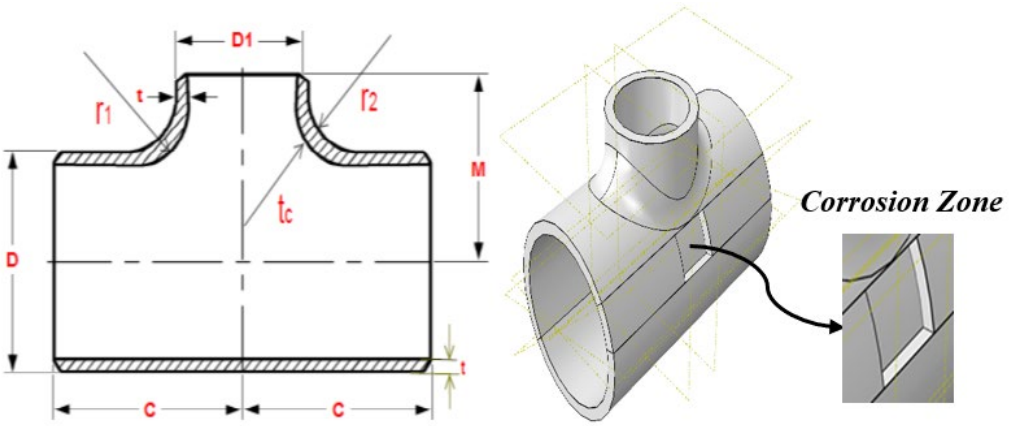

Fig. 1. ASME B16.9 Reducing Tee.

NPS inch	*O.D. (mm) D*	*O.D. (mm) D1*	*Center to End (mm) C*	*Center to End (mm) M*	*Thickness (mm) t*
6 - 4	*168.3*	*114.3*	*143*	*130*	*10.97*
	Crotch Radius (mm) r_1	*Crotch Radius (mm) r_2*	*Crotch Thickness (mm) t_c*		
	20	*30*	*11.6*		

Table 1. Geometric dimensions of the structure.

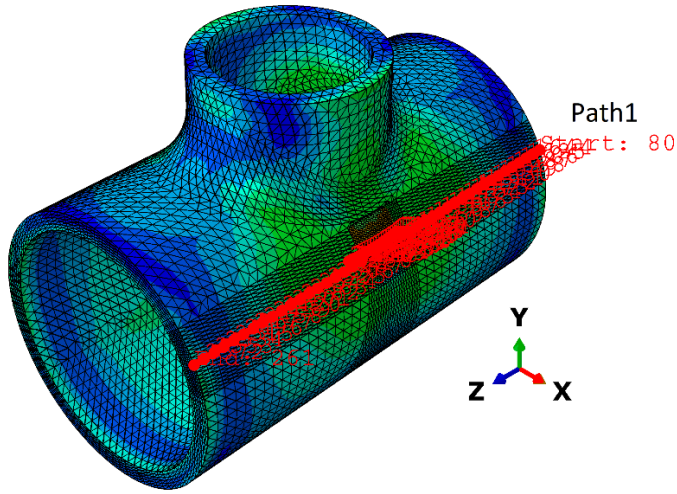

Fig.2. Study pathway.

The mechanical properties of the steel used in this study are listed in Table 2.

Material	***Properties***			
	Linear (Below Yield)		***Nonlinear (Above Yield)***	
			Yield stress	***Plastic strain***
ASTM A106 Grade B	*Young's Modulus*	*207 GPa*	*301*	*0.0000*
	Poisson's Ratio	*0.3*	*317*	*0.0029*
			374	*0.0138*
			412	*0.0207*
			482	*0.0386*
			534	*0.0575*
			596	*0.0862*
			648	*0.1222*

Table 2. Mechanical properties of ASME B16.9 reducing tee steel (Chen et al. 2021).

3. Boundary Conditions for Welding Reducing Tee (Inlet & Outlet)

A section of the welding reducing tee was cut in the circumferential direction to simulate realistic constraints during finite element analysis. Both the inlet and outlet ends were fully fixed.

Applied Constraints:

Displacement: U1=U2=U3=0

Rotation: UR1=UR2=UR3=0

The applied load is represented by internal pressure acting on the inner surface of the pipe tee.

This setup ensures that all translational and rotational degrees of freedom are blocked at both ends, allowing for accurate stress distribution analysis within the tee structure. Figure 3 illustrates the boundary conditions of the welded reducing tee.

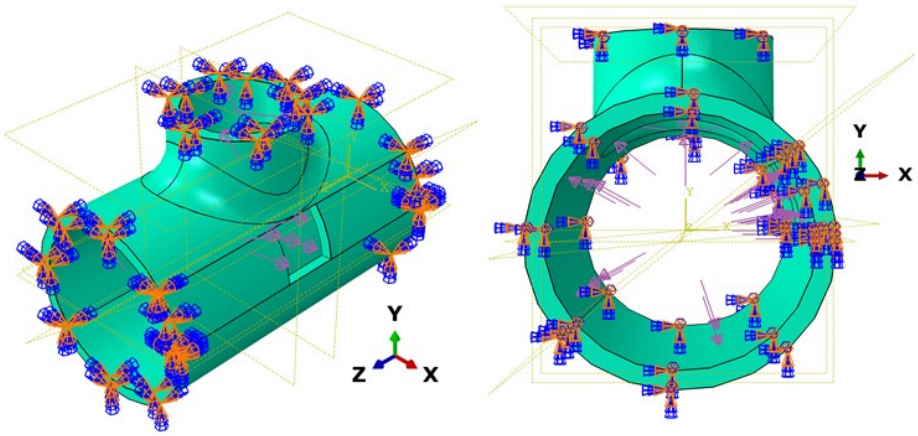

Fig. 3. Boundary conditions of the welding reducing tee.

4. Mesh Configuration for Welding Reducing Tee Analysis

4.1. Non-corrosive Structure

The finite element model was discretized using a uniform mesh to ensure consistency across all simulation cases. A fixed mesh configuration was maintained throughout the analysis to guarantee numerical stability and allow direct comparison of the results, as illustrated in Figure 4. The global mesh size was approximately 6 mm, and the geometry was meshed exclusively with C3D4 four-node linear tetrahedral elements, which are well-suited for complex pressure-containing components. The final mesh consisted of 12,589 nodes and 49,063 elements, all of which were of type C3D4. This mesh density provided adequate resolution to accurately capture localized stress gradients, particularly within the crotch radius, and the transition zones surrounding the branch outlet of the tee.

4.2. Corrosive structure

The structural model was discretized using a uniform global mesh size of approximately 6 mm to ensure consistent spatial resolution across the computational domain. This mesh configuration was maintained for all simulation cases to preserve numerical stability and allow reliable comparison of results, except within the defect region where enhanced accuracy was required. In this critical zone, a locally refined mesh—with an element size of roughly 2 mm—was implemented to more effectively capture steep stress gradients, as depicted in Figure 4. Such localized refinement is essential for accurately resolving the stress concentrations that typically develop around the defect, the weld toe, and the crotch radius. The defect itself was modeled as a rectangular region measuring 50 mm × 40 mm with a depth of 10 mm. The final discretized model comprised 18,277 nodes and 72,811 elements, all of which were C3D4 four-node linear tetrahedral elements, selected for their suitability in representing complex geometries and localized stress fields. This meshing strategy provides a robust basis for evaluating the structural integrity of the pipe connection under operational loading conditions.

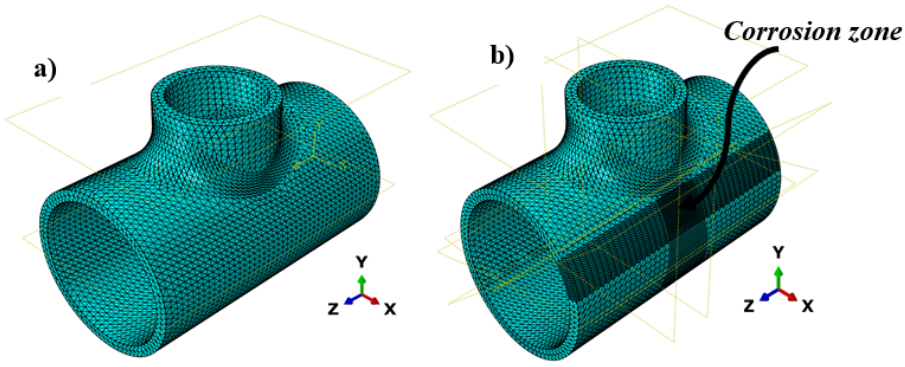

Fig. 4. Refined mesh applied to the numerical model of the pipe tee: a) Non-corrosive structure; b) Corrosive structure.

5. Results and discussion

5.1. Validation of results

Figure 5 presents a comparative analysis between the finite element method (FEM) stress–strain response and the experimentally derived stress–strain curve (Duell et al. 2008). Both curves exhibit the characteristic non-linear relationship between stress and strain, reflecting the elastic–plastic behavior of the material. At low strain levels, the FEM prediction closely follows the experimental data, accurately capturing the sharp increase in stress associated with the onset of plastic deformation. As strain increases, the FEM curve continues to align well with the experimental response. However, minor deviations are observed, particularly in the intermediate plastic range, where the FEM slightly underestimates stress levels. Nonetheless, the overall correspondence remains strong at higher strains, where both approaches converge—indicating reliable modeling of material hardening behavior. The close agreement between FEM predictions and the experimental stress–strain relationship confirms the robustness of the numerical model in reproducing the material's deformation characteristics. This validation supports its suitability for subsequent simulations involving complex loading conditions, reinforcing confidence in its predictive capacity for structural integrity assessments.

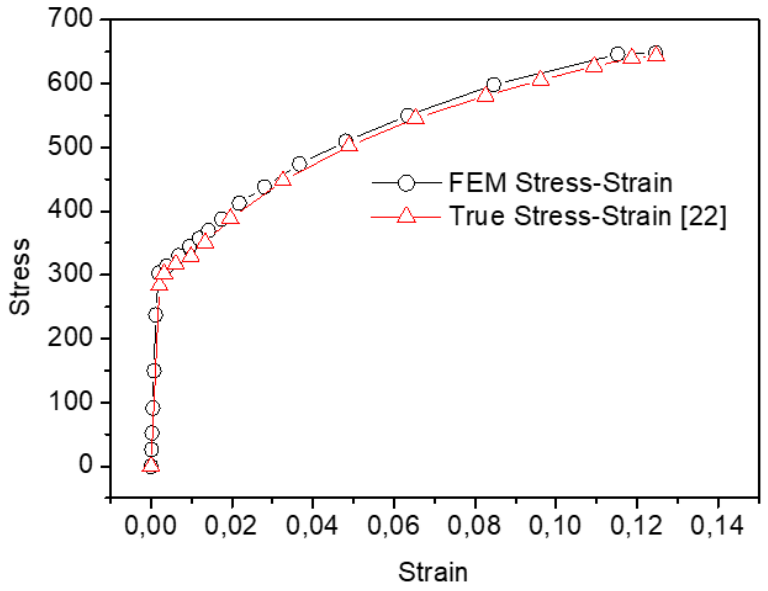

Fig. 5. FEM stress-strain results are compared with the experimental data.

5.2. Effect of internal pressure

This section of the study presents a numerical analysis of the effect of internal pressure applied to a branched pipe containing an external rectangular defect, focusing on the magnitude and distribution of equivalent stresses induced within the structure using the finite element method. The results, illustrated in Figure 6, show the distribution and evolution of equivalent Von Mises stresses under internal pressures of 10, 20, and 30 MPa. These stresses were computed along Path 1, schematically represented in Figure 2. For a pipe tee with a rectangular corrosion defect located beneath the crotch, the curves in Figure 6 reveal that internal pressure predominantly amplifies tangential stresses. The circumferential (hoop) stress (Fig. 6a) is the most critical, reaching the highest values, as it represents the principal stress generated by internal pressure in cylindrical geometries and is highly sensitive to pressure increases. The longitudinal stress (Fig. 6b) follows a similar trend but with lower magnitudes, resulting from axial equilibrium imposed by the applied pressure and the geometry of the component. The radial stress (Fig. 6c) remains the lowest; although directly related to the applied pressure, it consistently remains inferior to the tangential stresses. Minor fluctuations are observed near the defect edges, attributable to geometric discontinuities. The equivalent Von Mises stress (Fig. 6d) exhibits two distinct peaks localised at the edges of the defect, reflecting stress concentration effects due to the localised loss of wall thickness. The intensity of these peaks increases almost proportionally with the applied internal pressure (10, 20, and 30 MPa), indicating predominantly linear-elastic behaviour and suggesting an increasing risk of plastic deformation or crack initiation in these critical areas. Outside the defective region, stress levels remain relatively low and uniform, confirming that corrosion constitutes the principal weakness in pressure-bearing assessment.

It can therefore be deduced that peaks in Von Mises, circumferential, and longitudinal stresses occur precisely around the corrosion defect. Corrosion reduces the effective wall thickness, thereby diminishing the resistant cross-section available to withstand internal pressure, which leads to elevated local stresses. In other words, corrosion acts as a stress concentrator,

making these regions the most susceptible to plastic deformation or crack initiation under higher pressures.

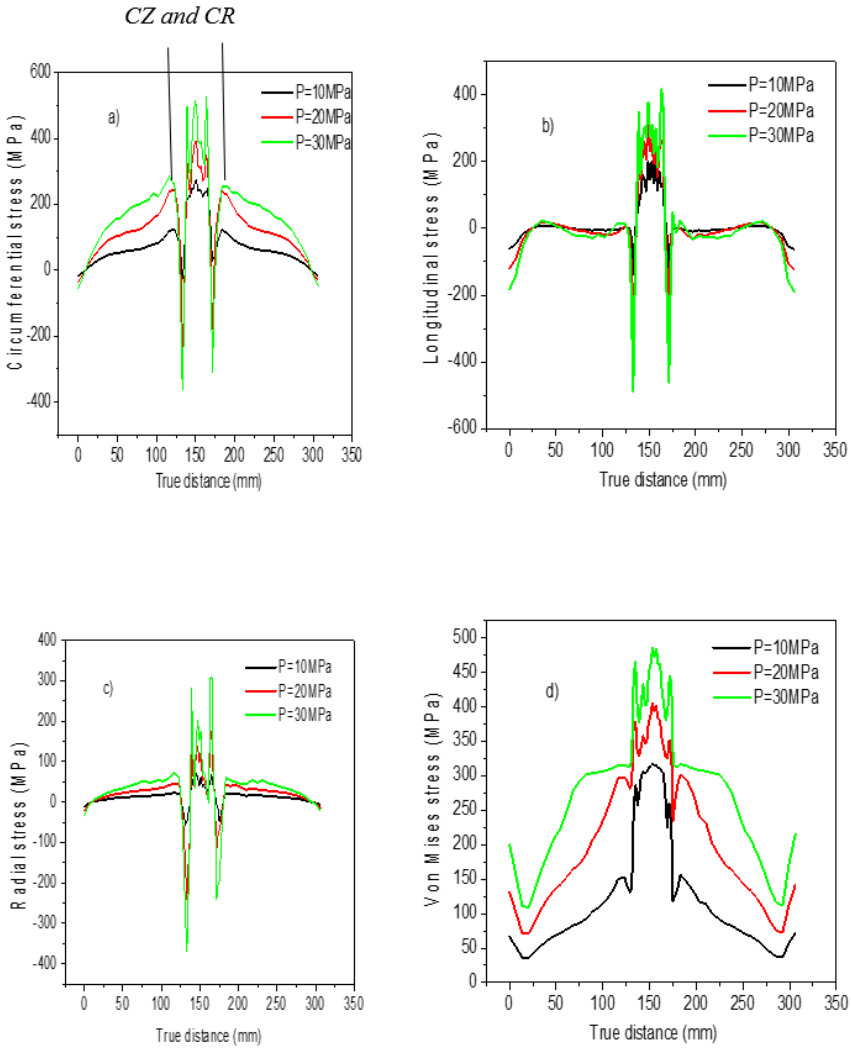

Fig. 6. Variation of Von Mises and principal stresses as a function of internal pressure along Path1

5.3. Comparative Analysis

Finite element analysis offers a powerful method for evaluating the distribution of equivalent Von Mises stresses in T-junctions subjected to internal pressure. Figure 7 compares the evolution of these stresses across two distinct configurations: a defect-free, compliant tee and a tee containing a localised defect. This comparison underscores the significant impact of geometric imperfections on the mechanical response of the structure under varying internal pressures (10, 20, and 30 MPa).

In the defect-free tee (Figure 7a), stresses are primarily concentrated at the junction between the branch and the main body, with magnitudes increasing proportionally to the applied pressure.

At 30 MPa, although stresses approach critical levels, their distribution remains relatively uniform around the junction, indicating stable stress transfer across the geometry. In contrast, the presence of a local defect (Figure 7b) results in a much more pronounced stress concentration. Even under a modest internal pressure of 10 MPa, a localised region of high stress emerges, becoming progressively more critical as pressure increases. These findings illustrate the inherent sensitivity of T-junctions to geometric defects. Such imperfections act as stress raisers and potential crack initiators, significantly reducing mechanical strength and limiting the service life of pressurised connections.

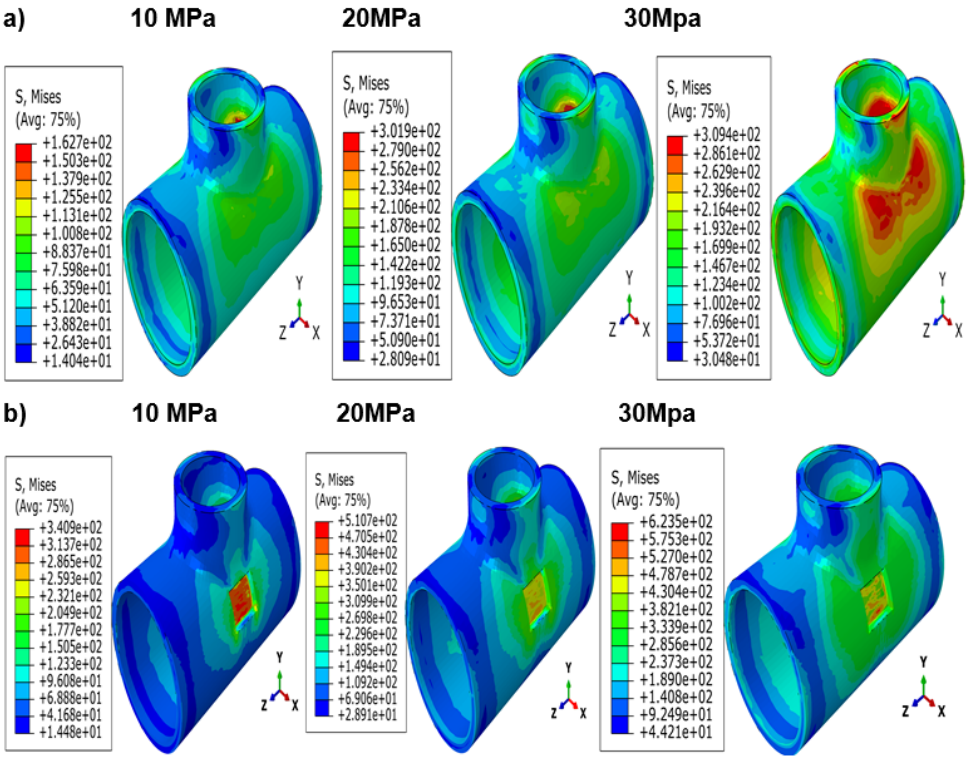

Fig. 7. Von Mises equivalent stress levels as a function of internal pressure: (a) Tee without a corrosion defect; (b) Tee with a corrosion defect.

5.4. Depth–spacing interaction effect

The investigation of the interaction between defect depth and spacing is essential for understanding their combined influence on stress distribution in a pipe tee. While each parameter individually affects the intensity of the equivalent Von Mises stress, their combined effect can significantly amplify localised stress concentrations, thereby undermining the overall mechanical resistance of the structure. In this study, Von Mises stress was evaluated for various defect spacings (d = 5, 10, 20, 40, 60, and 80 mm) and depths (h = 2, 4, 6, 8, and 10 mm). The results illustrated in Figure 8 clearly show that maximum stress is concentrated at the centre of the corrosion defect. This section presents the effect of the interaction between two centred rectangular corrosion defects located outside the welding region of a reducing tee, focusing on the level and distribution of equivalent stress generated as a function of defect depth and applied internal pressure. Comparable findings were reported (Metehri et al. 2018), who conducted a similar investigation into the influence of crack interactions on stress intensity factors in SiC

particle-reinforced Aluminium composites. Their results reinforce the significance of defect geometry and spacing in governing local stress amplification and structural reliability.

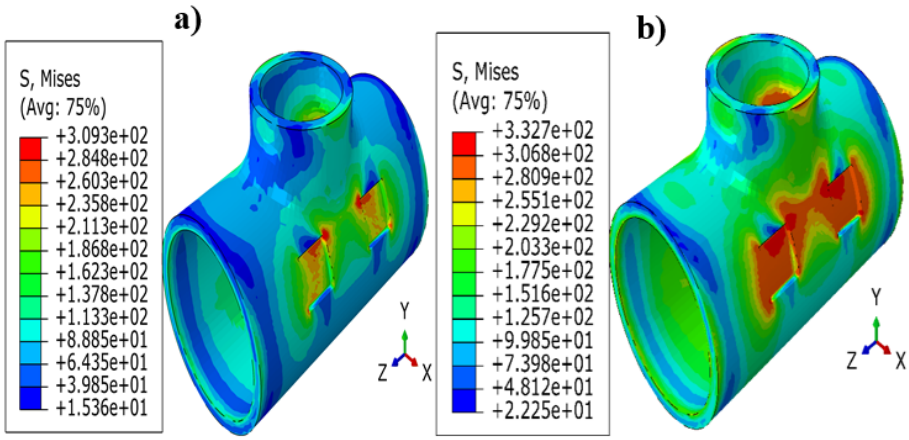

Fig. 8. Von Mises stress contours in the reducer tee with two neighboring corrosion defects under internal pressure: (a) P=15 MPa; (b) P=25 MPa.

Figure 8 shows the distribution of this equivalent stress and its intensity for P = 15- 25 MPa, defect depth h = 10 mm, and a is the distance between the corrosion defects, with d = 60 mm.

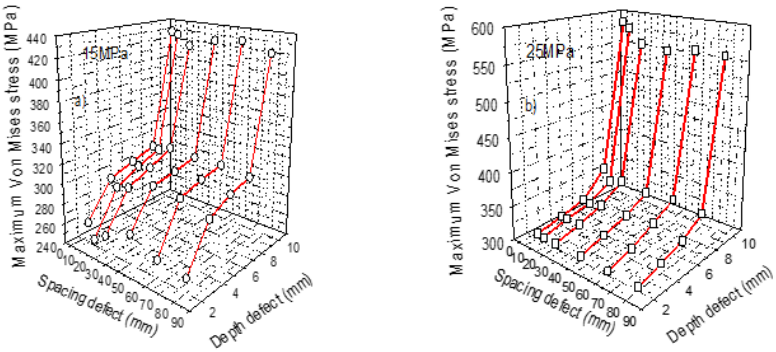

Fig. 9. Maximum Von Mises stress in relation to the corrosion defect depth and spacing in the reducer pipe **tee** (a) P=15 MPa; (b) P=25 MPa.

Figure 9a demonstrates that the maximum equivalent Von Mises stress in the steel pipe tee increases significantly with corrosion defect depth, particularly when two rectangular corrosion defects are located in close proximity. For small spacings (10–30mm), the interaction between the stress fields generated by each defect leads to pronounced concentrations, rapidly reaching elevated values (exceeding 400 MPa) once the defect depth surpasses 8 mm. Conversely, when the spacing is larger (≥60 mm), the mutual influence of the defects diminishes, and the stress stabilises at lower levels (approximately 250–320 MPa), even for comparatively deep defects. Therefore, the most critical condition for the structural integrity of the pipe tee arises from the

combined effect of significant defect depth and reduced spacing. Figure 9b provides a similar interpretation but reveals an additional amplification of the equivalent stresses, rising from around 400 MPa to nearly 600 MPa. This suggests that, in the second case (likely subjected to a higher internal pressure of 25 MPa), the structure experiences an even more severe concentration of stresses. The associated damage ratio is calculated at 146% for the first case and 199% for the second, clearly exceeding the material's yield limit. Such results highlight a significant risk of fracture or severe structural damage.

5.5. The Effect of Crotch Thickness and Radius

As part of the mechanical assessment of reducing tees in compliance with ASME B16.9, it is essential to analyze the influence of geometric parameters on stress concentration at the crotch region. The numerical study carried out enables the observation of the variation in maximum equivalent Von Mises stresses as a function of the fillet radius and local thickness under a service internal pressure of 15 MPa. In Figure 10, the distribution of the equivalent Von Mises stresses in the reducing tee subjected to an internal pressure of 15 MPa is shown for two different values of residual thickness at the crotch (t_c).

This Figure clearly illustrates the combined influence of the residual thickness t_c and the crotch radii r_1 and r_2 on the mechanical behaviour of a reducing tee subjected to an internal pressure of 15 MPa. In case (a), where $r_1 = 20$ mm and $r_2 = 0$ with a relatively small residual thickness ($t_c = 7.23$ mm), the presence of a sharp edge on the r_2 side produces a pronounced stress concentration, thereby increasing the vulnerability to localised damage. By contrast, in case (b), where $r_1 = 0$ and $r_2 = 20$ mm with a larger thickness ($t_c = 13.66$ mm), the 20 mm radius smooths the geometric transition, enabling a more uniform redistribution of stresses. As a result, the Von Mises peaks are reduced, and the overall structural performance is improved.

These observations demonstrate that increasing t_c in combination with a softened radius significantly mitigates stress concentrations. At the same time, a sharp edge powerfully amplifies the risk of crack initiation and local plastic deformation. Under an internal pressure of 15 MPa, and taking $\sigma_{ult} = 648$ MPa, the Von Mises peaks are approximately 260 MPa for case (a), corresponding to ≈40.1% of σ_{ult}, and 289 MPa for case (b), corresponding to ≈44.59% of σ_{ult}. Hence, increasing residual thickness and incorporating a 20 mm crotch radius on the critical side lowers stress peaks (and thus the damage ratio), whereas a sharp edge ($r = 0$) intensifies stress concentration.

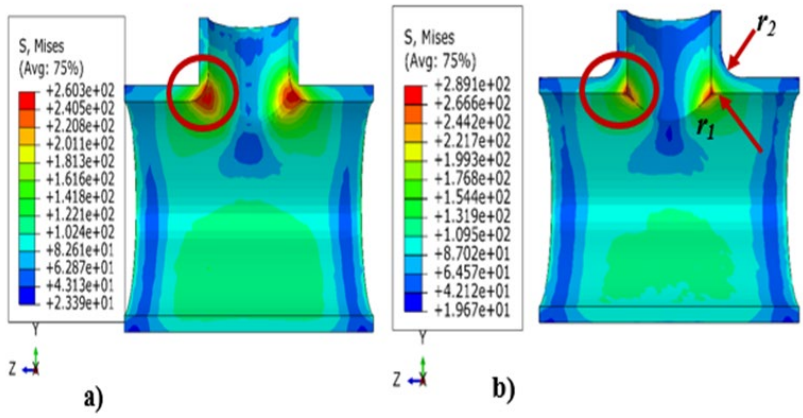

Fig. 10. Von Mises equivalent stress levels as a function of 15MPa internal pressure, crotch radius, and crotch thickness: a) r_1=20mm, r_2=0, tc= 7.23mm, and b) r_1=0, r_2=20mm, tc= 13.66mm.

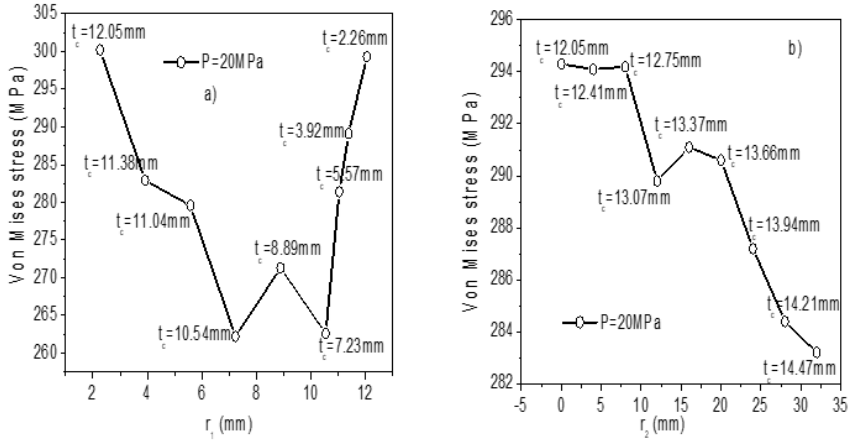

Fig. 11. Maximum Von Mises stress variation in the reducer pipe tee as a function of crotch radius and thickness: P= 20MPa.

Figure 11 illustrates the variation of the maximum equivalent Von Mises stress in a reducing tee subjected to an internal pressure of 20 MPa, as a function of the fillet radius (r_1), the external radius (r_2), and the local thickness (t_c). The analysis highlights the significant influence of geometry on stress distribution. At P = 20 MPa, Figure 11a (variation of the internal fillet radius, r_1) shows that as r_1 increases from approximately 2 to 12 mm, the Von Mises stress decreases from about 305 MPa to 262 MPa, corresponding to a reduction of nearly 14% (with a minimum around $r_1 \approx 10$–12 mm depending on the local thickness t_c). Figure 11b (variation of the external radius, r_2) reveals a more moderate effect: as r_2 increases from about 0 to 30 mm, the stress decreases from ~294 MPa to ~283 MPa, i.e., by about 4%. In summary, increasing r_1 is clearly more effective in reducing stress peaks (≈ three times the effect of r_2), while increasing r_2 provides an additional but less significant benefit. The annotations of t_c confirm that local thickness also

influences the stress level, but the dominant trend remains a reduction in stresses with increasing r_1, and to a lesser extent, r_2. These results demonstrate that the fillet radius is the most decisive factor in lowering stresses at the tee crotch. At the same time, the wall thickness acts as a secondary yet complementary parameter in enhancing the mechanical safety of the component, as noted in this study (Chinh and Long. 2023).

5.6. Size defect

In this study, the finite element method was employed to evaluate the equivalent Von Mises stresses in three models of varying sizes but with identical defect geometry and depth ($c = 10$ *mm*). The defect dimensions were as follows: Model 1 ($a = 40$ *mm,* $b = 50$ *mm*), Model 2 ($a = 50$ *mm,* $b = 60$ *mm*), and Model 3 ($a = 60$ *mm,* $b = 70$ *mm*). Internal pressure ranged from 15 to 20 MPa, depending on the case considered. The results were obtained by plotting the stress distribution along path 1 (Fig. 2)

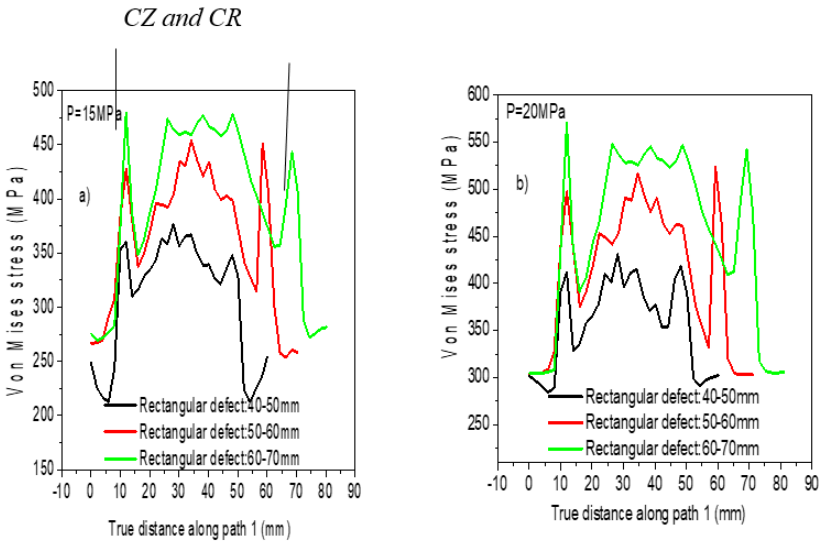

Fig. 12. Variation of Von Mises stress in the reducer pipe tee as a function of corrosion defect size.

From the curves in Figure 12 (a, b), it is evident that the Von Mises stress increases with both the applied internal pressure and the defect size. At P = 15 MPa, the maximum stress for the smallest defect (*40×50 mm*) is approximately 320 MPa, increasing to nearly 420 MPa for the medium defect (*50×60 mm*, i.e., +31%) and exceeding 480 MPa for the most significant defect (*60×70 mm*, i.e., +50% relative to the smallest one). At P = 20 MPa, a similar trend is observed: the minor defect reaches about 380 MPa, the medium defect around 500 MPa (+32%), and the most significant defect nearly 560 MPa (+47%). Overall, these results clearly demonstrate that, for a constant depth, an increase in defect size markedly amplifies the local stress by nearly half compared to the smallest defect, and that this amplification remains consistent across both pressure levels.

6. Conclusion

This study investigates the structural behavior of a steel reducing pipe tee with a rectangular defect located beneath the crotch area under internal pressure. Finite element simulations were employed to evaluate the residual stress distributions resulting from the applied boundary conditions, with a particular focus on the combined effects of the defect and crotch geometry—both identified as critical points for stress concentration and potential crack initiation. A comprehensive set of parametric studies was conducted to assess the impact of key factors, including internal pressure, defect dimensions, crotch radius, crotch thickness configurations, and the interaction between defect depth and spacing. These parameters were carefully selected to reflect conditions directly relevant to the design and integrity assessment of pressure-bearing pipe connections. Based on these investigations, the following main conclusions can be drawn:

- The findings confirm that internal pressure has a direct and proportional impact on the equivalent Von Mises stresses. As pressure increases, stress levels rise significantly, accelerating the risk of local yielding in critical areas. This demonstrates that internal pressure is a primary loading parameter governing the mechanical response and structural integrity of the component.
- The analysis indicates that the interaction between corrosion defect depth and spacing plays a crucial role in stress amplification. When defects are deeper and positioned closer together, local stress levels increase significantly compared to isolated or shallow defects, indicating a strong synergistic effect. This interaction underscores the importance of simultaneously considering both depth and spacing when evaluating the severity of corrosion damage and ensuring structural integrity.
- The fillet radius and local wall thickness at the crotch region are critical in stress mitigation. Increasing the internal fillet radius significantly reduces peak stresses, while the wall thickness provides additional, albeit secondary, reinforcement. These findings highlight the importance of optimized geometry in enhancing the mechanical integrity and service life of reducing tees under internal pressure.
- The study shows that corrosion defect size significantly impacts stress distribution. For a constant defect depth, increasing the defect dimensions leads to a marked rise in equivalent Von Mises stresses—up to nearly 50% higher compared to the smallest defect. This demonstrates that defect size is a critical parameter governing the severity of local stresses and, consequently, the structural integrity of the component.

Nomenclature and Abbreviations

FEA: Finite element analysis.
CZ: Corrosion zone
CR: Crotch region
d: Inter-defect distance (mm)
$\boldsymbol{E}$: Young modulus (GPa)
$\boldsymbol{\upsilon}$: Poisson coefficient
P: Internal pressure (MPa)
h: Depth of defect (mm)
S Mises: Von Mises stress (equivalent stress) (MPa)
$\mathbf{S_{11}} = \boldsymbol{\sigma_{xx}}$**:** Radial stress (MPa)
$\mathbf{S_{22}} = \boldsymbol{\sigma_{yy}}$: Circumferential stress (MPa)
$\mathbf{S_{33}} = \boldsymbol{\sigma_{zz}}$**:** Longitudinal stress (MPa)

References:

Chen, J., Wang, H., Salemi, M., & Balaguru, P. N. (2021). Finite element analysis of composite repair for damaged steel pipeline. Coatings, 11(3), 301. https://doi.org/10.3390/coatings11030301.

Chen, S. S., Wang, H. X., Jiang, H., Liu, Y. N., Liu, Y. X., & Lv, X. X. (2020). Risk assessment of corroded casing based on analytic hierarchy process and fuzzy comprehensive evaluation. Petroleum Science, 1–12. https://doi.org/10.1007/s12182-020-00507-0.

Chinh, V. D., & Long, D. T. (2023). Corrosion effect on stress concentration factor in tubular T-joints under axial loading. Journal of Structural Construction Engineering (JSTCE), 17(3), 154–165. https://doi.org/10.31814/stce.huce2023-17(3)-12.

Duell, J. M., Wilson, J. M., & Kessler, M. R. (2008). Analysis of a carbon composite overwrap pipeline repair system. International Journal of Pressure Vessels and Piping, 85(11), 782–788. https://doi.org/10.1016/j.ijpvp.2008.08.001.

Fezazi, A. I., Mechab, B., Salem, M., & Serier, B. (2021). Numerical prediction of the ductile damage for axial cracks in pipe under internal pressure. Frattura ed Integrità Strutturale, 15(58), 231–241. https://doi.org/10.3221/IGF-ESIS.58.17.

Huang, Y., Qin, G., & Yang, M. (2023). A risk-based approach to inspection planning for pipelines considering the coupling effect of corrosion and dents. Process Safety and Environmental Protection, 180, 588–600. https://doi.org/10.1016/j.psep.2023.10.025.

Ibrahim, N. C. M., Serier, B., & Mechab, B. (2018). Analysis of the crack-crack interaction effect initiated in aeronautical structures and repaired by composite patch. Frattura ed Integrità Strutturale, 12(46), 140–149. https://doi.org/10.3221/IGF-ESIS.46.14.

Kim, Y.-J., Park, K.-H., & Lee, J.-H. (2021). Corrosion effects on crack growth in pipelines: A numerical approach. Corrosion Science, 186, 109449. https://doi.org/10.1016/j.corsci.2021.109449.

Kim, Y. J., Shim, D. J., Huh, N.-S., & Kim, Y.-J. (2002). Plastic limit pressures for cracked pipes using finite element limit analyses. International Journal of Pressure Vessels and Piping, 79(5), 321–330. https://doi.org/10.1016/S0308-0161(02)00031-5.

Maachou, S., Mechab, B., Bachir Bouiadjra, B., & Salem, M. (2025). Using fatigue analysis to predict the propagation of internal and external semi-elliptical cracks in pipes under cyclic load. Journal of Pressure Vessel Technology, 147(6), 061702. https://doi.org/10.1115/1.4069008.

Mechab, B., Benouar, A., Bachir Bouiadjra, B., Salem, M., & Kaddouri, K. (2025). Plastic limit of repaired steel pipe elbow with bonded composite wrap. Journal of Pressure Vessel Technology, 147(6), 061302. https://doi.org/10.1115/1.4068953.

Mechab, B., Chioukh, N., Mechab, B., & Serier, B. (2018). Probabilistic fracture mechanics for analysis of longitudinal cracks in pipes under internal pressure. Journal of Failure Analysis and Prevention, 18, 1643–1651. https://doi.org/10.1007/s11668-018-0564-8.

Mechab, B., Salem, M., Medjahdi, M., & Serier, B. (2020). Probabilistic elastic-plastic fracture mechanics analysis of propagation of cracks in pipes under internal pressure. Frattura ed Integrità Strutturale, 14(54), 202–210. https://doi.org/10.3221/IGF-ESIS.54.15.

Mechab, B., Serier, B., Bachir Bouiadjra, B. A., Kaddouri, K., & Feaugas, X. (2011). Linear & non-linear analyses for semi-elliptical surface cracks in pipes under bending. International Journal of Pressure Vessels and Piping, 88(1), 57–63. https://doi.org/10.1016/j.ijpvp.2010.11.001.

Mechab, B., Serier, B., Kaddouri, K., & Bachir Bouiadjra, B. A. (2014). Probabilistic elastic-plastic analysis of cracked pipes subjected to internal pressure loads. Nuclear Engineering and Design, 275, 281–286. https://doi.org/10.1016/j.nucengdes.2014.05.008.

Metehri, A., Kouider Madani, & Raul, D. S. G. Campliho. (2024c). Numerical analysis of the geometrical modifications effects on the tensile strength of bonded single-lap joints.

International Journal of Adhesion and Adhesives, 134, 103814. https://doi.org/10.1016/j.ijadhadh.2024.103814.

Metehri, A., Madani, K., & Lousdad, A. (2018). Effect of crack position and particle size on SIF in SiC-reinforced Al composite. Frattura ed Integrità Strutturale, 48, 152–160. https://doi.org/10.3221/IGF-ESIS.48.18.

Metehri, A., Madani, K., Mechab, B., Mokhtari, M., & Ghermaoui, I. M. A. (2024b). Tensile examination of progressive damage in porous ceramic composite using XFEM. Military Technical Courier, 72(3). https://doi.org/10.5937/vojtehg72-50091.

Metehri, A., Mechab, B., & Bachir Bouiadjra, B. (2024a). Predicting burst pressure in corroded pipes under internal pressure. Military Technical Courier, 72(4), 1747–1771. https://doi.org/10.5937/vojtehg72-50357.

Metehri, A., Mechab, B., & Bachir Bouiadjra, B. (2025). Using the finite element method for developing a new model predicting the burst pressure of straight defects in corroded pipes repaired with bonded composite wraps. Military Technical Courier, 73(3), 917–941. https://doi.org/10.5937/vojtehg73-56344.

Metehri, A., Serier, B., Belhouari, M., & Mecirdi, M. A. (2009). Numerical analysis of the residual stresses in polymer matrix composites. Materials & Design, 30(7), 2332–2338. https://doi.org/10.1016/j.matdes.2008.11.009.

Salem, M., Mechab, B., Berrahou, M., Bachir Bouiadjra, B. A., & Serier, B. (2019). Failure analyses of propagation of cracks in repaired pipes. Journal of Failure Analysis and Prevention, 19, 212–218. https://doi.org/10.1007/s11668-019-00592-3.

Salem, M., Mhamdia, R., Mechab, B., & Bachir Bouiadjra, B. (2024). Effect of the stiffness ratio on the growth of repaired fatigue cracks with composite patch. Mechanics Based Design of Structures and Machines, 52(5), 2679–2697. https://doi.org/10.1080/15397734.2023.2189941.

Serier, N., Mechab, B., Mhamdia, R., & Serier, B. (2016). A new formulation of the J integral of bonded composite repair in aircraft structures. Structural Engineering and Mechanics: An International Journal, 58(5), 745–755. https://doi.org/10.12989/sem.2016.58.5.745.

Talbi, S., Salem, M., Mechab, B., Ghomari, T., Allem, A., Bachir Bouiadjra, B., & Benelmaarouf, M. (2024). New investigation of delamination using the VCCT method to predict the damage in bonded composite repair plates subjected to tensile load. International Journal of Structural Integrity, 15(1), 1757–9864. https://doi.org/10.1108/IJSI-11-2023-0113.

Tang, X., Yang, Y., & Li, J. (2020). Advances in structural health monitoring for pipeline systems. Sensors, 20(18), 5278.

Taylor, C., Das, S., Collins, L., & Rashid, M. (2017). Fatigue crack growth at ERW seam of API 5L X-70 steel. Journal of Offshore Mechanics and Arctic Engineering, 139(3), 031401. https://doi.org/10.1115/1.4035385.

Wang, Y., & Xu, F. (2021). Real time monitoring systems for pipeline crack detection: A review. Sensors, 21(8), 2782. https://doi.org/10.3390/s21082782.

Wasim, M., & Djukic, M. B. (2022). External corrosion of oil & gas pipelines: Review of mechanisms and prevention. Journal of Natural Gas Science and Engineering, 100, 104467. http://dx.doi.org/10.1016/j.jngse.2022.104467.

Zhao, H., Liang, X., Yang, Z., He, P., & Zhao, B. (2024). Impact of corrosion on failure pressure of API 5L X65 pipeline. Journal of Marine Science and Engineering, 12(10), 1810. https://doi.org/10.3390/jmse12101810.

Zhao, W., Zhang, T., Wang, Y., Qiao, J., & Wang, Z. (2018). Corrosion failure mechanism of associated gas transmission pipeline. Materials, 11(10), 1935. https://doi.org/10.3390/ma11101935.